remote sensing

MDPI

Communication

A Demonstration of Three-Satellite Stereo Winds

James L. Carr [1,*], Jaime Daniels [2], Dong L. Wu [3], Wayne Bresky [4] and Bin Tan [5]

[1] Carr Astronautics, 6404 Ivy Lane, Suite 333, Greenbelt, MD 20770, USA
[2] NOAA/NESDIS Center for Satellite Applications and Research, College Park, MD 20740, USA
[3] NASA Goddard Space Flight Center, Greenbelt, MD 20770, USA
[4] I.M. Systems Group (IMSG), Rockville, MD 20852, USA
[5] Science System and Applications Inc., Lanham, MD 20706, USA
* Correspondence: jcarr@carrastro.com

Abstract: Stereo tracking of clouds from multiple satellites permits the simultaneous retrieval of an atmospheric motion vector ("wind") and its height in the atmosphere. The direct measurement of height is a major advantage of stereo methods over observations made from a single satellite where the height must be inferred from infrared brightness temperatures. A pair of operational geostationary satellites over the Americas provides stereo coverage where their two fields of view intersect. Stereo coverage can be extended to nearly a full hemisphere with a third satellite. We demonstrate this configuration with the operational GOES-R constellation of GOES-16 (east) and GOES-17 (west) augmented by GOES-18 in its central test slot and use the 500-m resolution Advanced Baseline Imager Band 2. We examine the consistency of the pairwise products created from GOES-18 and -16 versus GOES-18 and -17 and create a fused triple-GOES product that spans nearly the full hemisphere seen from GOES-18. We also examine the retrieval of ground points observed under clear skies and compare their retrievals to zero speed and known terrain heights. The results are compatible with a wind accuracy about 0.1 m/s with height assignment uncertainty of 175 m.

Keywords: atmospheric motion vectors (AMVs); GOES-R; ABI; stereo imaging; parallax; image navigation and registration (INR)

Citation: Carr, J.L.; Daniels, J.; Wu, D.L.; Bresky, W.; Tan, B. A Demonstration of Three-Satellite Stereo Winds. *Remote Sens.* **2022**, *14*, 5290. https://doi.org/10.3390/rs14215290

Academic Editors: Alexander Kokhanovsky, Dmitry Efremenko and Xiaofeng Yang

Received: 10 August 2022
Accepted: 13 October 2022
Published: 22 October 2022

1. Introduction

Stereo observing provides a means of retrieving wind vectors while simultaneously retrieving their height in the atmosphere using a pair of Geostationary (GEO) satellites [1,2] or a GEO and a Low-Earth Orbiting (LEO) satellite [3]. The general satellite-winds method does not require synchronized observing, only that pixel times are known or can be accurately modeled. Direct retrieval of geometric height is the primary advantage of the stereo-winds method. Satellite winds determined from a single observational platform must be assigned a height based on the infrared brightness temperatures of cloud tracers and thermodynamic modeling of the air column [4–11]. This can be the most important error source in a satellite wind product, particularly in the presence of inversions [12]. NOAA's Geostationary Operational Environmental Satellites R-series (GOES-R) constellation allows for persistent coverage of the Americas and surrounding oceans, but persistent stereo coverage is limited to where the fields of view of the two operational GOES-R satellites intersect. The stereo coverage area can be augmented by adding other sensors from LEO satellites or international partner GEO satellites. However, having a third operating GOES-R satellite can provide stereo coverage across almost an entire hemisphere. The post-launch testing of GOES-18 presented such an opportunity thanks its positioning at an 89.5°W test longitude with GOES-16 to its east at 75.2°W and GOES-17 to its west at 137.2°W. This paper takes advantage of this opportunity to demonstrate stereo winds for a three-satellite constellation using the Advanced Baseline Imager (ABI) Band 2, and compares the stereo products from the pairwise configurations of GOES-18 with either GOES-16 or -17.

2. Materials and Methods

A series of engineering tests are performed at the beginning of every GOES satellite mission aimed at setting up the system in its operational configuration and verifying its readiness to begin its operational lifetime. These include setup for the Image Navigation and Registration (INR) of the ABI. INR is critical for accurate stereo-wind retrievals as INR enables stable tracking and accurate assignment of apparent geographic locations to cloud tracers. The INR for the GOES-18 ABI Visible and Near Infrared (VNIR) bands achieved close to nominal performance in early May 2022. INR performance is assessed using the Image Navigation and Registration Performance Assessment Tool Set (IPATS) [13]. IPATS compares more than 600 locations of landmarks in the ABI imagery against Landsat reference templates remapped into the ABI fixed grid and measures navigation errors in the East–West (EW) and North–South (NS) directions. For each GOES image, the mean and the standard deviation of the good quality INR measurements are used to represent the INR performance that is shown in Figure 1. The GOES-R specifications require that the absolute value of the mean plus three times the sigma be less than 21 μradians. Achieving nominal INR performance for the ABI mid- and long-wave IR bands was planned for after the drift of GOES-18 to 136.8°W, a location too close to GOES-17 to be useful for stereo observing, and for this reason, only ABI Band 2 (B02), the 0.5 km resolution red channel, is demonstrated here.

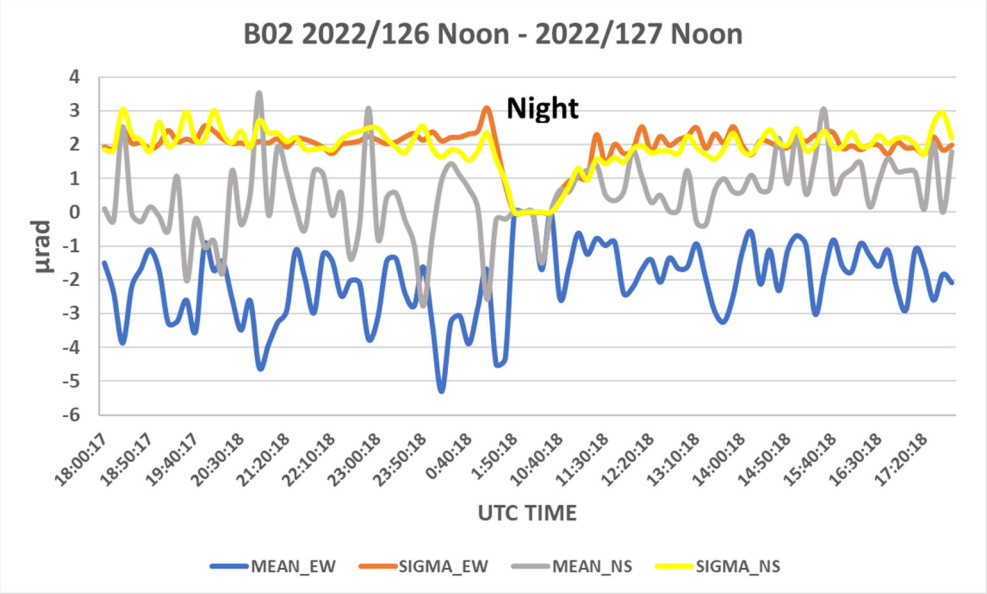

Figure 1. Landmark Measurements of GOES-18 INR Performance. Statistics show measured INR residual error in units of μradians for fully or partially illuminated ABI Full Disk scenes on 6 May 2022 for Band 2 plotted in chronological order and labeled by the Universal Time Coordinated (UTC) of the scene. Note: GOES-18 Preliminary, Non-Operational Data.

We take feature templates from a Full Disk (FD) image acquired by GOES-18. Features are tracked using template matching to find that feature in a preceeding and a following repetition of the GOES-18 FD and also two repetitions of the FD from either GOES-16 or -17, which have been remapped into the ABI fixed grid for GOES-18. The observed apparent shifts of features are called "disparities". Disparities between FD refreshes of GOES-18 measure atmospheric motion only, but disparities measured between satellites represent a combination of motion and geometric parallax due to height. The simulataneous retreival of both the wind and the height is possible knowing the pixel acquistion times.

Stereo winds were produced in the overlapping regions between GOES-18 and -16 and GOES-18 and -17 and then merged to provide a stereo winds product across the entire GOES-18 Full Disk. Figure 2 shows the retrieval sites for an 18:00Z Full Disk case.

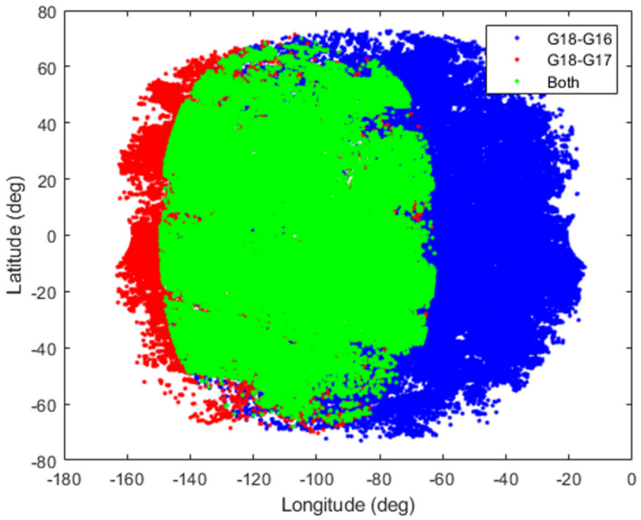

Figure 2. Sites for Stereo Wind Retrievals. Sites that are triple covered are shown in green.

Stereo winds were retrieved using science code [1] developed under NASA/GSFC and NOAA/STAR sponsorship and used to support work by NESDIS/STAR Winds Science Team towards development of operational stereo-wind products for GOES-GOES, GOES-Himawari, and other combinations including single and tandem VIIRS. The method does not require synchronization between observing systems and therefore is well suited to heterogeneous constellations. It should also be possible to retrieve wind vectors and heights using stereo observations from both pairings simultaneously in the region of triple coverage. However, merging after pairwise retrievals provides an opportunity to assess the consistency between the stereo wind products created from the individual pairings.

3. Results

The fused stereo winds product, shown in Figure 3, includes sites covered both doubly and triply by the three-satellite GEO constellation. Figure 3 retrievals have been thinned and superimposed over a Band 2 18:00Z context image.

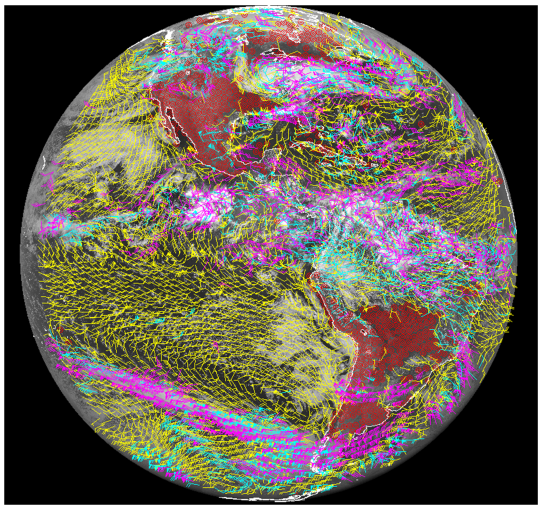

Figure 3. Three-Satellite Stereo Winds across the Full Disk of GOES-18 (Band 2, 18:00Z on 6 May 2022). The wind barbs are color coded to indicate retrieved geometric height (0–3000 m, yellow, 3000–7000 m, cyan, 7000–16,000 m, magenta). The wind barbs have been thinned to remove overlapping values and calm winds (ground points) are plotted in red. There are 380,179 high-quality retrievals in this dataset before thinning. Ground point retrieved heights can be compared with a digital terrain model to provide an indication of the accuracies of the retrieved geometric heights. Note: GOES-18 Preliminary, Non-Operational Data.

All results, including those in Figure 3, are included in the Supplementary Materials.

4. Discussion

Comparison between colocated GOES-18 plus -16 and GOES-18 plus -17 stereo wind products shows remarkable agreement between the two pairings (Figure 4).

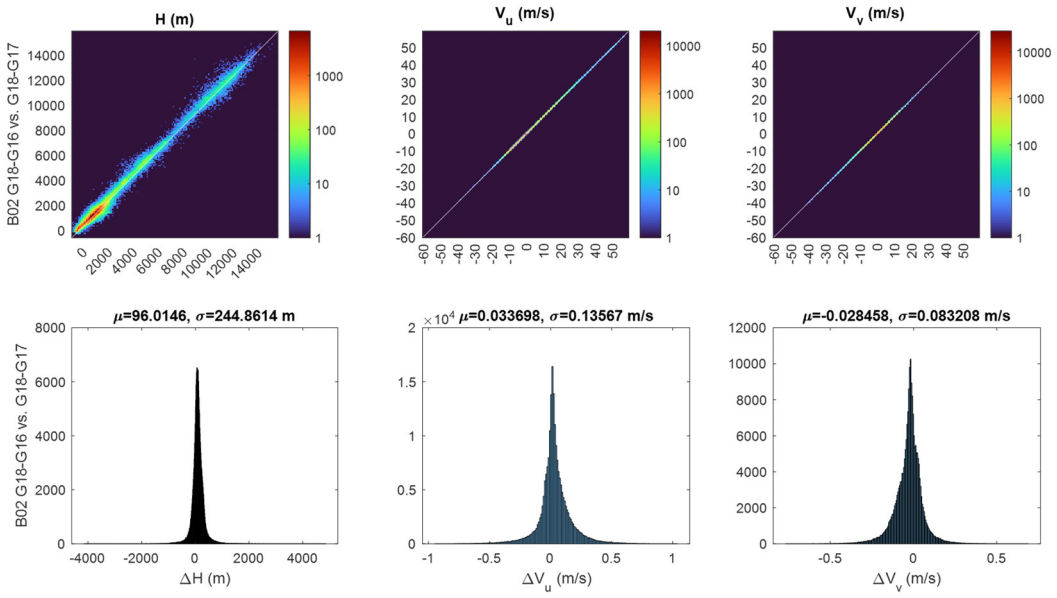

Figure 4. Log-density plots of GOES-18 plus -17 versus GOES-18 plus -16 Stereo-Wind Retrievals where there is Triple Coverage. There are N = 212,304 colocated retrievals in the difference histograms. If the retrieval errors were independent with similar statistics for each pairing, then the difference statistics would be consistent with individual statistics that are $1/\sqrt{2}$ of the sigma of the difference statistics, i.e., two-satellite retrieved height uncertainty <175 m and wind velocity uncertainty <0.1 m/s. Note: GOES-18 Preliminary, Non-Operational Data.

The stereo-wind science code also tracks ground features as if they were winds when skies are clear, some of which have been included in Figure 4 and identified as "calm winds". Ground-point statistics are indicative of the accuracy of the wind retrievals, most likely representing a lower bound since the error associated with representing the wind with cloud motion ("representativeness" error) is not included [14]. Figure 5 shows the ground-point statistics for the merged product in Figure 3 and a summary of the ground point statistics appears in Table 1. These statistics are compatible with the individual pairing statistics implied by the comparison of retrievals at all common sites (i.e., retrieved height uncertainty <175 m and wind velocity uncertainty <0.1 m/s).

Table 1. Ground Point Retrieval Statistics. Means (μ) and standard deviations (σ) from a sample size N are calculated with respect the ground truth of the GLOBE digital terrain model. The measured motion with respect to stationary ground is resolved relative to east- and north-pointing directions (u and v). Note: GOES-18 Preliminary, Non-Operational Data.

	N	$\mu(h)$	$\sigma(h)$	$\mu(V_u)$	$\sigma(V_u)$	$\mu(V_v)$	$\sigma(V_v)$
	-	m	m	m/s	m/s	m/s	m/s
G18 + 16	42,815	−104	150	0.01	0.04	−0.01	0.05
G18 + 17	25,453	39	133	0.02	0.07	−0.04	0.04
Merged	43,501	2	147	0.01	0.05	−0.02	0.05

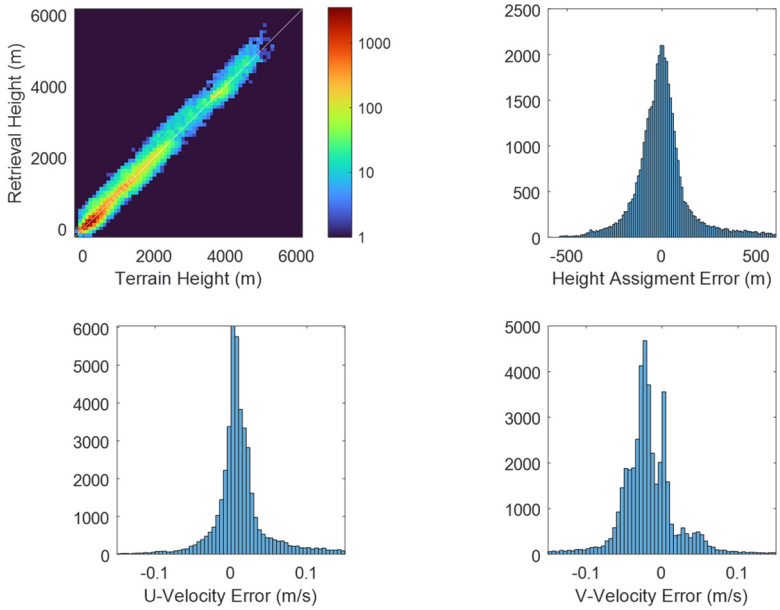

Figure 5. Ground-Point Retrieval Errors for the Merged Stereo Wind Product. Small height assignment biases, as indicated in Table 1, have been corrected in the merged product. Note: GOES-18 Preliminary, Non-Operational Data.

The performance of the stereo-wind algorithm can be further examined by looking at colocated retrieval consistency statistics in different layers: ground, low-level winds (0–3000 m), mid-level winds (3000–7000 m), and upper-level winds (7000–16,000 m). Ground points are identified by two-dimensional K-means clustering of height above terrain versus speed. Those retrievals not belonging to the ground class are considered winds that have been measured as a result of the stereo tracking of cloud, rather than terrain, features. Table 2 presents deviation statistics for one pairing (GOES-16/18) relative to the mean of both pairings.

Table 2. Retrieval Consistency Statistics. Note: GOES-18 Preliminary, Non-Operational Data.

	N	$\mu(h)$	$\sigma(h)$	$\mu(V_u)$	$\sigma(V_u)$	$\mu(V_v)$	$\sigma(V_v)$
	-	m	m	m/s	m/s	m/s	m/s
Ground	25,875	−6	67	−0.01	0.04	0.01	0.02
Lower	164,970	35	93	−0.02	0.06	0.02	0.04
Mid	10,723	−42	223	−0.02	0.12	0.01	0.06
Upper	10,736	−16	306	0.02	0.12	0.02	0.07
All	212,304	23	122	−0.02	0.07	0.01	0.04

Retrievals are most plentiful in the lower atmosphere, dominating the comparison statitistics across all heights. It is clear from Table 2 that there is a trend towards larger height uncertainty as the alititude increases.

5. Conclusions

Triple-GEO stereo from the GOES-R constellation brings stereo winds coverage to a full hemisphere which brings opportunities for enhancing the utility of these observations in operational numerical weather prediction and weather forecasting. The demonstration here could be repeated once GOES-18 becomes the operational western satellite and GOES-17 occupies the storage slot at 105°W and it is periodically exercised to maintain its operational readiness. A repeat demonstration with GOES-17 in the storage slot will permit examination of IR winds as well as visible-channel winds. ABI Band 14 (B14) is generally used for IR winds, which allows for full diurnal coverage of wind observations regardless of solar

illumination. Because of the coarser pixel resolution, it is expected that the ground-point and comparison statistics for B14 would be larger than those for B02. However, the growth will likely be sublinear with resolution, as was seen in a previous study of ground-point statistics using B02, B07, and B14 [1].

The consistency between the individually paired stereo datasets demonstrates the power of the stereo method. The results are compatible with a wind accuracy on the order of 0.1 m/s with height assignment uncertainty of 175 m across all altitudes but with an increasing trend with altitude. Similar uncertainties are revealed in the analysis of ground points under clear skies. The latter does not include representativeness error or the difference between cloud motion and air parcel motion as would be observed by a rawinsonde. Further investigation of the trends with layer height should be undertaken, particularly with a larger collection of stereo products.

The triple-GEO configuration should be considered as a future GEO constellation design since a third satellite in the constellation shows a signficant benefit for stereo wind coverage. The stereo-wind algorithm does not require synchronized sampling by the three GEO satellites as its time model takes into count any sampling time differences.

It is also worth noting the fact that high-quality stereo products can be generated from the GOES-18 plus -16 pairing where there is only a 14.3° separation in longitude. This result should be relevant for Asian satellite operators using instruments similar to ABI. Their satellites are presently located at 140.7°E (Himawari-8) and 128.2°E (GEO-KOMPSAT-2a), which have 12.5° separation.

Supplementary Materials: The following supporting information can be downloaded at: https://www.mdpi.com/article/10.3390/rs14215290/s1, stereo winds product files in netCDF format.

Author Contributions: Conceptualization, J.D., D.L.W. and J.L.C.; methodology, J.L.C.; software, J.L.C., W.B., and B.T.; validation, J.L.C., and B.T.; formal analysis, J.L.C.; investigation, J.L.C.; resources, J.D. and D.L.W.; data curation, J.L.C.; writing—original draft preparation, J.L.C., W.B. and B.T.; writing—review and editing, J.D. and D.L.W.; visualization, W.B.; supervision, J.D.; project administration, J.D.; funding acquisition, J.D. and D.L.W. All authors have read and agreed to the published version of the manuscript.

Funding: This research and APC were funded by NOAA/STAR under contract number STI330-I7-CQ-0052, TO 2, Atmospheric Science and Technology Applications (ASTA). Additional funding for science code development was provided by NASA Goddard Space Flight Center under the NNG17HP01C contract through Support for Atmospheres, Modeling, and Data Assimilation (SAMDA). IPATS development and use was supported by NASA under the Hydrospheric and Biospheric Science (HBS) Support Services contract at NASA Goddard Space Flight Center (NNG15HG01C). ASTA is managed by I.M. Systems Group (IMSG). SAMDA and HBS are managed by Science Systems and Applications, Inc. (SSAI).

Conflicts of Interest: The authors declare no conflict of interest.

References

1. Carr, J.L.; Wu, D.L.; Daniels, J.; Friberg, M.D.; Bresky, W.; Madani, H. GEO–GEO Stereo-Tracking of Atmospheric Motion Vectors (AMVs) from the Geostationary Ring. *Remote Sens.* **2020**, *12*, 3779. [CrossRef]
2. Lee, J.; Shin, D.-B.; Chung, C.-Y.; Kim, J. A Cloud Top-Height Retrieval Algorithm Using Simultaneous Observations from the Himawari-8 and FY-2E Satellites. *Remote Sens.* **2020**, *12*, 1953. [CrossRef]
3. Carr, J.L.; Wu, D.L.; Wolfe, R.; Madani, H.; Lin, G.; Tan, B. Joint 3D-Wind Retrievals with Stereoscopic Views from MODIS and GOES. *Remote Sens.* **2019**, *11*, 2100. [CrossRef]
4. Menzel, W.P.; Smith, W.L.; Stewart, T.R. Improved Cloud Motion Wind Vector and Altitude Assignment Using VAS. *J. Clim. Appl. Meteorol.* **1983**, *22*, 377–384. [CrossRef]
5. Szejwach, G. Determination of Semi-Transparent Cirrus Cloud Temperature from Infrared Radiances: Application to METEOSAT. *J. Appl. Meteorol.* **1982**, *21*, 384–393. [CrossRef]
6. Schmetz, J.; Holmlund, K.; Hoffman, J.; Strauss, B.; Mason, B.; Gaertner, V.; Koch, A.; Van De Berg, L. Operational Cloud-Motion Winds from Meteosat Infrared Images. *J. Appl. Meteorol.* **1993**, *32*, 1206–1225. [CrossRef]
7. Nieman, S.J.; Schmetz, J.; Menzel, W.P. A Comparison of Several Techniques to Assign Heights to Cloud Tracers. *J. Appl. Meteorol.* **1993**, *32*, 1559–1568. [CrossRef]

8. Frey, R.A.; Baum, B.A.; Menzel, W.P.; Ackerman, S.A.; Moeller, C.C.; Spinhirne, J.D. A comparison of cloud top heights computed from airborne lidar and MAS radiance data using CO_2 slicing. *J. Geophys. Res. Atmos.* **1999**, *104*, 24547–24555. [CrossRef]
9. Heidinger, A.K.; Pavolonis, M.J. Gazing at Cirrus Clouds for 25 Years through a Split Window. Part I: Methodology. *J. Appl. Meteorol. Clim.* **2009**, *48*, 1100–1116. [CrossRef]
10. Borde, R.; Doutriaux-Boucher, M.; Dew, G.; Carranza, M. A Direct Link between Feature Tracking and Height Assignment of Operational EUMETSAT Atmospheric Motion Vectors. *J. Atmos. Ocean. Technol.* **2014**, *31*, 33–46. [CrossRef]
11. Bresky, W.; Daniels, J.; Bailey, A.A.; Wanzong, S.T. New Methods toward Minimizing the Slow Speed Bias Associated with Atmospheric Motion Vectors. *J. Appl. Meteorol. Clim.* **2012**, *51*, 2137–2151. [CrossRef]
12. Velden, C.S.; Bedka, K.M. Identifying the Uncertainty in Determining Satellite-Derived Atmospheric Motion Vector Height Attribution. *J. Appl. Meteorol. Clim.* **2009**, *48*, 450–463. [CrossRef]
13. Tan, B.; Dellomo, J.J.; Folley, C.N.; Grycewicz, T.J.; Houchin, S.; Isaacson, P.J.; Johnson, P.D.; Porter, B.C.; Reth, A.D.; Thiyanratnam, P.; et al. GOES-R series image navigation and registration performance assessment tool set. *J. Appl. Remote Sens.* **2020**, *14*, 032405. [CrossRef]
14. Cordoba, M.; Dance, S.L.; Kelly, G.A.; Nichols, N.K.; Waller, J.A. Diagnosing atmospheric motion vector observation errors for an operational high-resolution data assimilation system. *Q. J. R. Meteorol. Soc.* **2016**, *143*, 333–341. [CrossRef]